One-Step Plasma Jet Deposition and Self-Sintering of Gold Nanoparticle Inks on Low-Temperature Substrates

Jacob Manzi[1], Tony Varghese [2,3], Josh Eixenberger [3,4], Lakshmi Prakasan[1], David Estrada [3-6], and Harish Subbaraman[1,6]*

***Abstract*—Flexible electronics on low-temperature substrates like paper are very appealing for their use in disposable and biocompatible electronic applications and areas like healthcare, wearables, and consumer electronics. Plasma-jet printing uses a dielectric barrier discharge plasma to focus aerosolized nanoparticles onto a target substrate. The same plasma can be used to change the properties of the printed material and even sinter *in situ.* In this work, we demonstrate one-step deposition of gold structures onto flexible and low-temperature substrates without the need for thermal or photonic post-processing. We also explore the plasma effect on the deposition of the gold nanoparticle ink. The plasma voltage is optimized for the sintering of the gold nanoparticles, and a simple procedure for manufacturing traces with increased adhesion and conductivity is presented, with a peak conductivity of 6.2 x10^5 S/m. PJP-printed gold LED interconnects and microheaters on flexible substrates are developed to demonstrate the potential of this single-step sintered deposition of conductive traces on low-temperature substrates.**

***Index Terms*—Additive manufacturing, plasma jet printing, flexible hybrid electronics, wearables.**

I. INTRODUCTION

FABRICATION of flexible devices using additive manufacturing has been rapidly increasing for several decades due to the low-cost, economical nature of the technology. Additive manufacturing has been used to demonstrate flexible devices such as opto-electronic devices, gas sensors, chemical sensors, phased-array antennas, radio frequency identification devices, and organic thin-film transistors using printing modalities such as inkjet and aerosol-jet printing [1], [2], [3], [4], [5], [6], [7], [8], [9], [10], [11], [12], [13], [14]. A wide variety of nanomaterial inks have been formulated for various additive printing techniques, including 2D and 3D printing applications [15], [16], [17]. The use of additive technologies is very attractive for the ability to fabricate conductive traces onto many types of substrates, including flexible substrates like polymers and papers. The global printed electronics market is expected to be propelled to over USD 44 billion by 2030, with applications in the automotive, biomedical, consumer electronics, smart packaging, defense, and aerospace industries[18]. While a rapidly developing technology, there are some challenges to address regarding the longevity of printed devices in sensitive, humid, or corrosive environments.

Metallic nanoparticles dispersed into a nanoparticle ink are commonly used for additive manufacturing of conductive traces [19], [20], [21]. These nanoparticles must be converted into conductive metal films by forming necks between the particles, removing any solvents, capping agents, and ink additives, while also densifying the nanoparticles into a continuous film. To achieve this, a post-processing step of sintering at high temperatures is usually used. Even with the reduction of nanoparticle size to achieve a lower melting temperature, sintering temperatures of over 200°C are not uncommon for silver and gold commercial inks, as well as long sintering times over 30-120 minutes [22], [23], [24], [25]. To obtain high conductivities, temperatures of 500°C and times of 300 minutes have been reported [22]. This is not ideal for heat-sensitive substrates such as paper and low glass-transition polymers that cannot withstand this treatment. Several solutions including laser, plasma, and intense pulsed light sintering, aim to address this problem. Laser sintering has the advantage of selective area sintering and local high temperatures[26]. The drawback is that a single laser beam sintering large areas can take significant time. Intense pulsed light uses the higher absorption of electromagnetic radiation of the metal particles compared to the

This paragraph of the first footnote will contain the date on which you submitted your paper for review, which is populated by IEEE. The authors acknowledge support from the NASA EPSCoR (grant # 80NSSC19M0151), NSF (award # CMMI-1825502) and Idaho Commerce IGEM (award# 3732018). We acknowledge infrastructure support from the Department of Energy Nuclear Science User Facilities General Infrastructure Program through award numbers DE-NE0008677. D.E. and J.E. acknowledge support from the Center for Advanced Energy Studies.

[1] School of Electrical Engineering and Computer Science, Oregon State University, Corvallis, OR 97331 USA
[2] Department of Electrical and Computer Engineering, Boise State University, Boise, ID 83725 USA
[3] Micron School of Material Science and Engineering, Boise State University, Boise, ID 83725 USA
[4] Center for Advanced Energy Studies, Boise State University, Boise, ID 83725 USA
[5] Idaho National Laboratory, Idaho Falls, ID 83415, USA
[6] INFlex labs LLC, Boise, Idaho, USA.
* Correspondence: harish.subbaraman@oregonstate.edu;

Color versions of one or more of the figures in this article are available online at http://ieeexplore.ieee.org

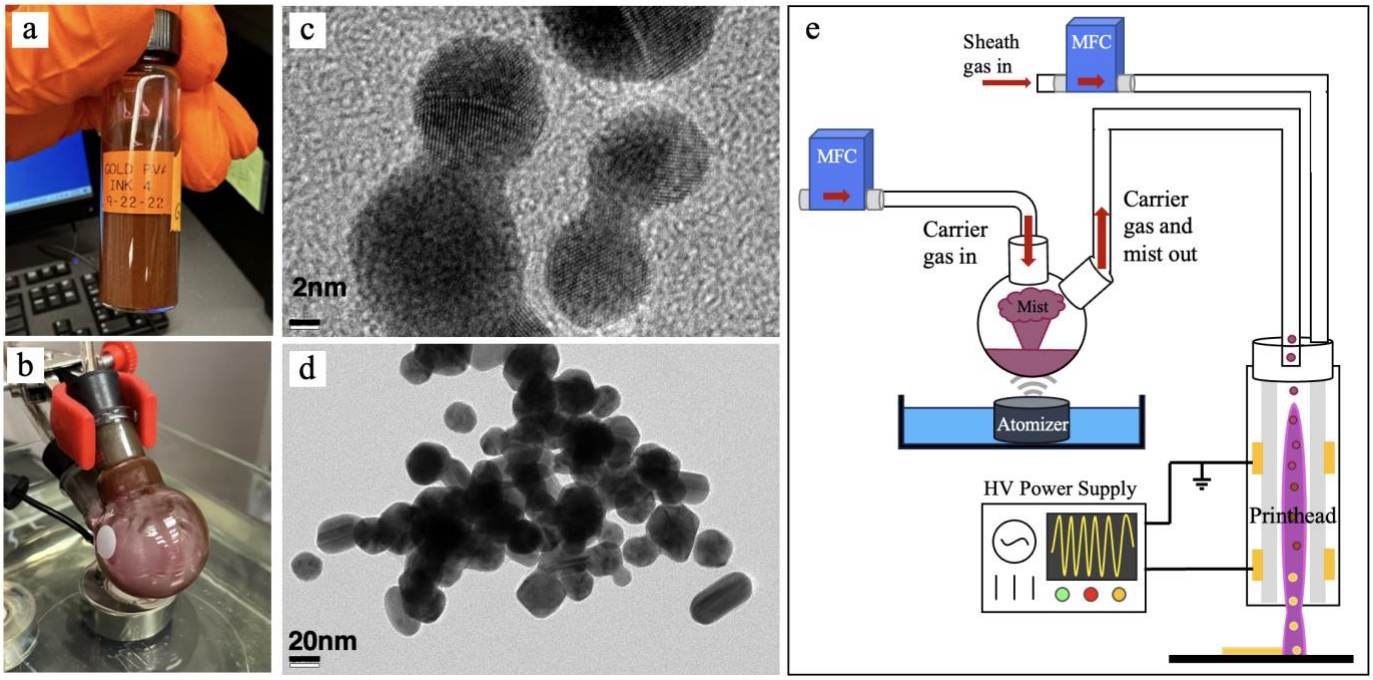

Fig. 1. (a) Gold nanoparticle ink dispersed in DI water. (b) Gold ink ultrasonic atomization in glass flask. (c) TEM of uncapped gold nanoparticles with 2nm scale bar and (d) 20nm scale bar. (e) Plasma jet printer schematic showing basic parts used for of plasma deposition.

surrounding substrate. This method can generate local temperatures of over 1000°C within the metal traces. The speed of pulsed light sintering can be much faster than laser sintering but can cause delamination problems as the temperature difference from the heated metal to the cooler substrate can generate significant thermal stress [27], [28]. Near-infrared (NIR) sintering can also be an effective approach to low-temperature sintering of nanoparticle inks [13]. With this method, rapid sintering is achievable but the ink must be tuned for NIR absorption. Plasma sintering is a good alternative to these methods and has been demonstrated by using low-pressure and atmospheric-pressure plasma to sinter conductive printed nanomaterial [29], [30]. Plasma sintering can affect small or large areas by changing the nozzle size or using a plasma chamber[29], [31], [32]. While low-pressure plasma sintering can have some problems with only sintering a "skin depth" these issues have not been observed with atmospheric-pressure plasma sintering, as will be highlighted later in this article [29], [31], [33].

Silver is commonly used as a conductor in printed electronics applications but has a drawback of oxidation in many environments and is not inherently biocompatible [34]. Oxidation will cause the drifting of sensors and reduce electronic function over time without passivation and could even result in device failure. Gold is a much more stable solution for certain applications in printed electronics where good conductivity is needed without the risk of oxidation. However, the sintering temperature of gold nanoparticles of even a few nanometers is reported to be up to 300 to 400ºC, which is incompatible with most low-temperature substrates [13], [35]. Additionally, regardless of sintering temperature, all jetting depositions of gold nanoparticles so far have required a two-step process— print and then sinter. In this work, we show the deposition of gold nanoparticles and *in situ* plasma sintering, which can be a single-step manufacturing process.

Plasma jet printing (PJP) is a unique printing technique that offers two major advantages over the more commonly used technologies such as inkjet and aerosol jet printing— (1) it can print independently of gravity, and (2) it can pattern self-sintered nanoparticle films *in situ* in a single step. Because the deposition flow depends on both the carrier gas pressure of the jet as well as the electromagnetic forces of the plasma, conductive traces can be printed in space and microgravity environments, enabling on-demand manufacturing of electronics for long-term space missions [31], [33], [36].

The plasma jet printhead comprises two ring electrodes around a ceramic dielectric connected to a high voltage (0-25kV), low-frequency (~27kHz) power supply. The applied voltage and frequency generate an atmospheric pressure, dielectric barrier discharge plasma. A nanoparticle ink is atomized by an ultrasonic transducer, and the mist is carried to the printhead via a helium carrier gas. As they pass through the plasma, the nanoparticles in the ink are bombarded by ions, electrons, electromagnetic radiation, and other species in the plasma. When properly tuned, this can result in solvent evaporation and sintering of the nanoparticle films during deposition, as plasma has been shown to sinter metal nanoparticle films [29]. This can cut out the expensive and time-consuming post-processing steps and enable direct manufacturing onto low-temperature substrates such as paper, low-glass transition polymers, and textiles for fabricating electronics and sensors for gas sensing and wearable health monitoring applications. A schematic of the plasma jet parts can be seen in Fig. 1e, showing helium gas flows, the ultrasonic atomization system, the printhead, and the power supply. An image of the PJP with the plasma plume is shown in Fig. 2a.

This work demonstrates a single-step plasma jet printing and sintering of flexible and conductive gold traces by leveraging the plasma printer's sintering abilities and ink modification. We show additively manufactured gold traces with superior adhesion onto flexible and low-temperature substrates. The gold ink was optimized experimentally for PJP, and lines were printed onto multiple substrates for characterization of the deposition. The plasma voltage and the number of passes were varied to observe the effect on the printed film quality. Optical and electron microscopy and electrical characterization were performed on the gold nanoparticle films.

II. Materials and Methods

2.1 Gold nanoparticle ink

Two gold nanoparticle inks were obtained from INFlex Labs, fabricated, and demonstrated for multijet deposition, i.e. multijet inks [13], [37]. In IFL_MJ-Au1, the synthesized nanoparticles were capped with polyvinylpyrrolidone (PVP) for suspension stability and resistance to agglomeration (Fig. 1a)[37]. These particles were suspended in deionized water. The second ink, IFL_MJ-Au2, contained gold nanoparticles with no polymer capping agent and simply consisted of the nanoparticles suspended in deionized water. The ink was diluted 10:1 with DI water and sonicated in a bath sonicator for 30 minutes before loading into the PJP for printing. Transmission electron microscopy (TEM) was performed on the gold nanoparticles to observe their size before printing. The TEM showed that the size of the particles is less than 60nm as shown in Fig. 1c and 1d, which is confirmed by our previous studies [37]. Full synthesis and materials characterization of the gold nanoparticles with PVP capping that were used in this ink can be found in ref. 37. The uncapped nanoparticles were synthesized without the PVP capping agent in a similar method. The crystalline nature of the gold nanoparticles can be observed in the higher-resolution TEM in Fig. 1c.

2.2 PJP Printing

The uncapped, IFL_MJ-Au2, gold ink PJP printing conditions were optimized by adjusting the sheath and precursor flow. For the IFL_MJ-Au2, the optimized sheath and precursor flows were found to be 350 SCCM and 100 SCCM, respectively, for a 1-2 mm printhead height above the substrate to minimize overspray and increase resolution. A customized ultrasonic atomizer was created using an ultrasonic transducer and a 50mL double-necked flask for continuous atomization of 2-3mL of gold ink. The ink atomizer is shown working in Fig. 1b where the red-colored gold ink is turned into a mist in the atomization flask. Lines were printed with varying plasma voltage to observe how the gold was deposited at different plasma powers. Since plasma has been shown to sinter materials while being deposited, we hypothesized that the gold could be sintered with the plasma [29], [32], [33], [36]. For characterization of the conductivity, a glass slide was used as rigid substrates are more consistent with using electrical characterization and microscopy before moving onto flexible substrates. The gold was deposited with varying plasma powers, which was controlled by adjusting the voltage of the AC power supply. Sets of lines were deposited at 10kV to 25 kV at intervals of 2.5kV to observe the effect of plasma voltage on the deposition, similar to Fig. 2(b). IFL_MJ-Au1 was also optimized and deposited with varying voltage on the commercial plasma jet printer.

2.3 Characterization

The resistance of each of the printed gold lines was measured using a four-point probe resistance measurement system or two-point resistance measurement system. The four-point system was used on the first samples to mitigate contact resistance from the probes. To calculate the resistivity, the cross-sectional area of the prints was measured using a profilometer (Bruker Dektak XT) by finding the width and average thickness of the printed lines. Scanning electron microscopy (SEM) images of samples printed at varying voltages were taken. Fig. 2c-d shows the printed uncapped gold showing significant grain growth of the gold nanoparticles in IFL_MJ-Au2 from their original size to a larger connected network.

III. Results

3.1 Plasma effect on conductivity

For the uncapped ink deposited from 10kV to 25kV, we measured an increase in average conductivity at 12.5kV. For higher deposition voltages between 15kV to 25kV, the conductivity of the printed gold film decreased, and the hypothesis of this will be explored in the following sections. Fig. 2e shows the average conductivity of printed lines at varying deposition voltages, with no post-processing. The most

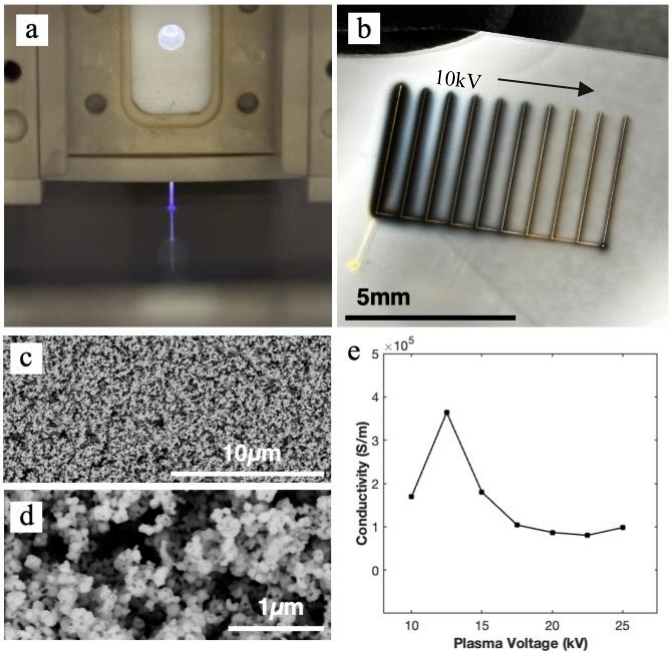

Fig. 2. (a) Photograph of plasma jet printer depositing onto glass. (b) gold lines printed at varying voltages onto glass. (c,d) Top-down SEM images of printed gold showing nanoparticle growth. (e) Conductivity of printed gold (IFL_MJ-Au2) lines vs. deposition plasma voltage.

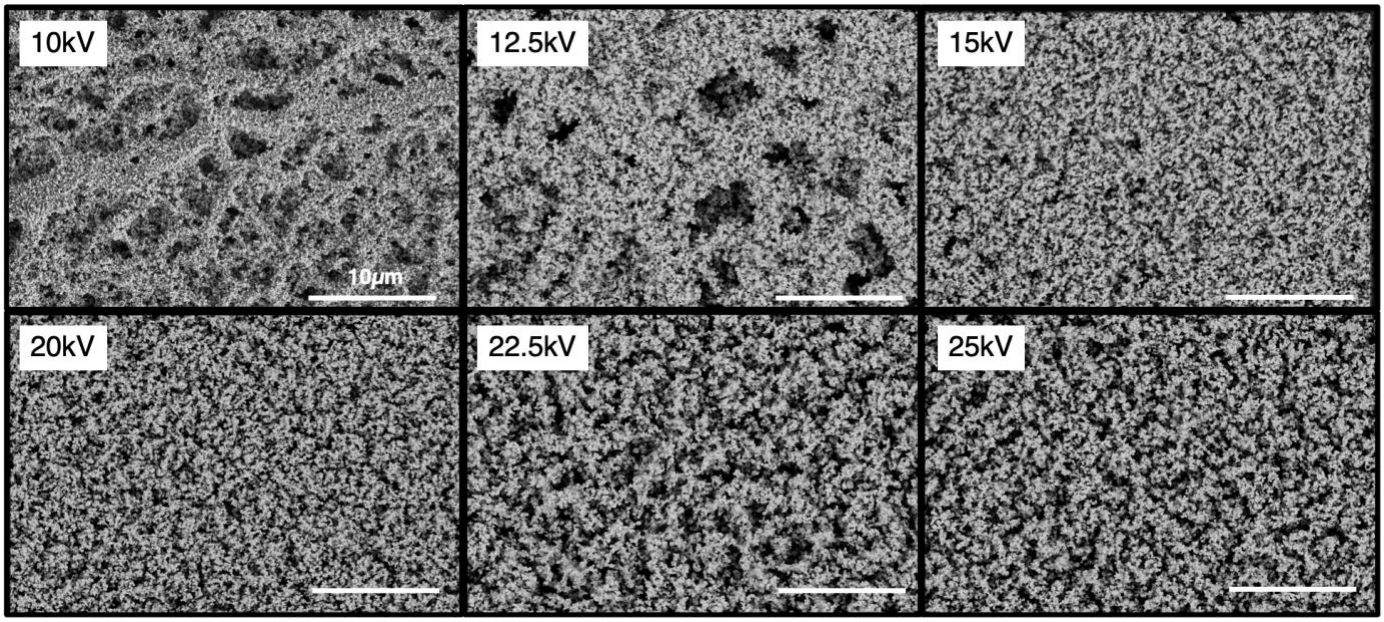

Fig. 3. Top-down SEM images of printed gold at varying deposition voltages showing varying deposition topography at different voltages and increasing porosity. All scale bars are 10um.

conductive gold line printed at 12.5kV peaked at 6.2 x10^5 S/m, which is about 65 times less than conductive bulk gold. Profilometer analysis of the cross-sectional area of all these films showed an average increase of 50% from 10kV to 15kV and a further decrease for higher voltages.

Another interesting observation comes from the SEM topography images of each plasma voltage. Non-ideal porosity is generated in films deposited at higher voltages. Fig. 3 shows that at 10kV, the particles are deposited with good packing density but exhibit little grain growth with large and small particles mixed together. When the voltage was increased to 12.5kV, many more of the smallest particles are sintered to form larger particles. At 15kV, the particle size remains similar, but the vertical porosity of the material increases. At 20kV and 25kV, the vertical porosity is further and significantly increased. The porosity of these films was quantified using area threshold masking, and it was observed that the porosity increases in the sample with increasing plasma voltage from 5% to 30%. The increased porosity is detrimental to the conductivity, as is observed with the decrease in conductivity for higher voltages. We are observing two effects as the uncapped gold is deposited—As the plasma power is increased, it delivers more energy to the nanoparticles and has the opportunity to further sinter them. Simultaneously, as plasma power increases it begins to introduce porosity in the films, and reduces the cross-sectional area. These work against each other so that there is an optimal deposition voltage for the uncapped ink that is 12.5kV, lower than the maximum explored. Additionally, as the plasma power increases, the deposition of the uncapped ink becomes less as the particles can be charged and can blow off of the substrate entirely. As seen the in Fig. 2b, the width of the printed line and overspray significantly decrease with increasing plasma voltage.

The polymer-capped ink (IFL_MJ-Au1) showed no conductivity with any deposition voltage, indicating that the plasma did not remove the polymer capping agent and the nanoparticles were not sintered together. The printed lines were carbon coated and observed in the SEM to confirm this. No necking of the particles was observed and the particles were significantly larger than their uncapped counterparts, which indicates the covering of each particle with the polymer. The morphology of the particles differs greatly from the uncapped ink.

3.2 Printed Electrodes

Electrodes were printed onto polyimide, paper, and other low-temperature substrates to demonstrate the ability of the PJP to deposit sintered gold onto low-temperature, flexible substrates (Fig. 4c). LEDs were attached to the electrodes with silver paste, it was cured at 50°C or by being left in air overnight, and

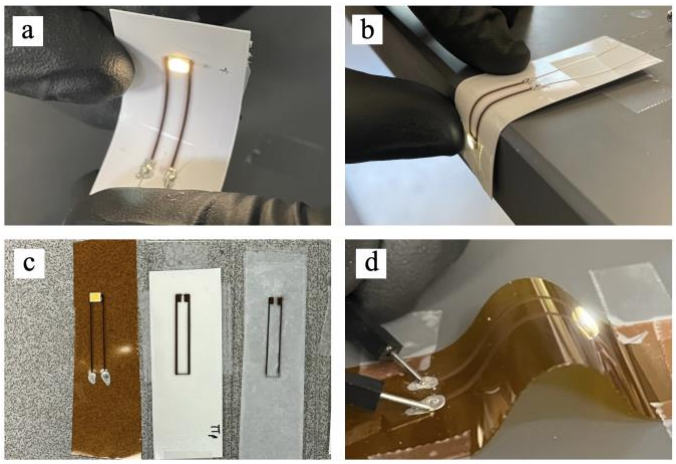

Fig 4. (a) gold electrodes deposited onto paper and flexed in hand, (b) in reverse direction over a table edge. (c) electrodes deposited onto polyimide, tattoo paper, and scotch tape. (d) Lighting of LED with 3V on polyimide while flexed.

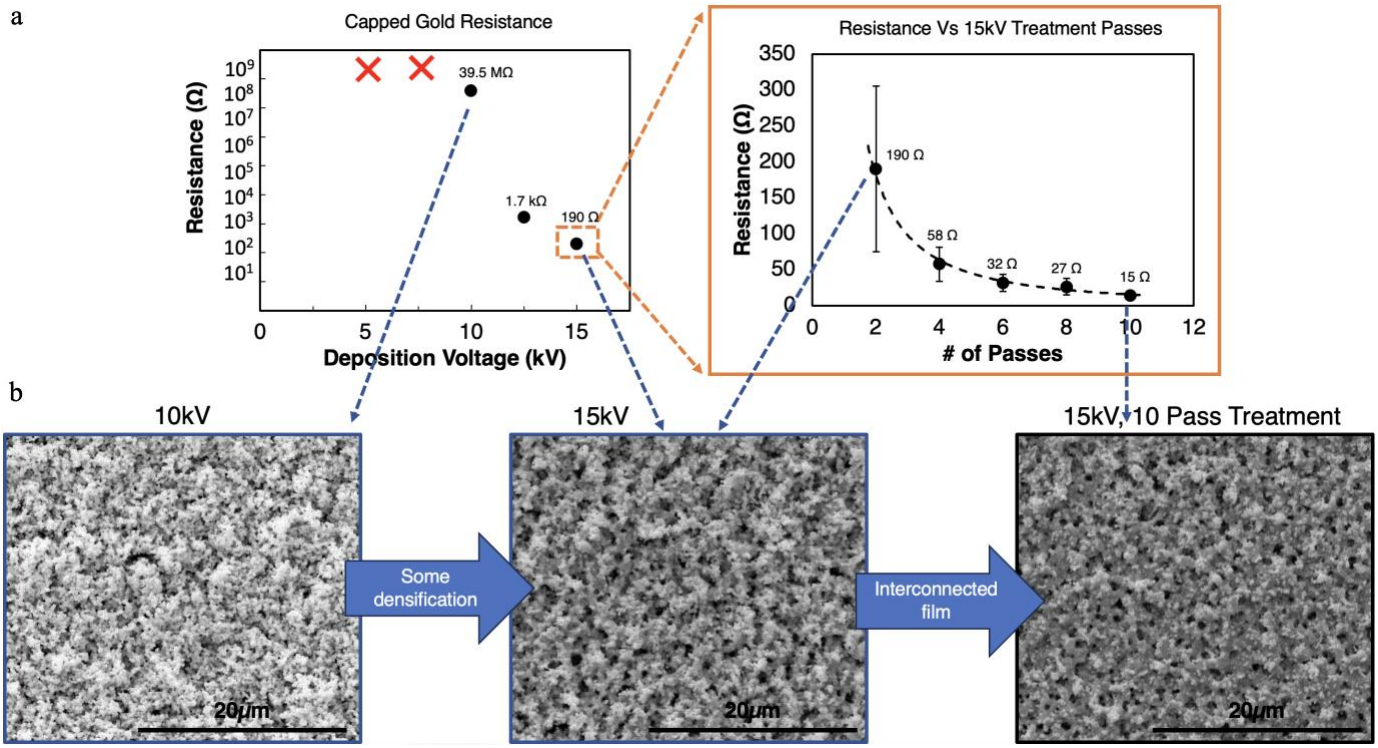

Fig 5. (a) Modified gold (IFL_MJ-Au3) resistance deposited by PJP on glass. Resistance of printed gold line vs post printing plasma treatment passes. (b) SEMs showing the densification and necking of gold nanoparticles with increased voltage and treatment.

the LEDs were powered on with as little as 3V. As demonstrated in Fig. 4(a)-(b), (d), the LED connection can be flexed on paper and polyimide in either direction, and no change in brightness was observed on the LED, indicating a strong connection and flexibility of the plasma-deposited gold electrodes.

3.3 Adhesion of uncapped gold

A common problem with additive manufacturing using gold is that gold has inherently poor adhesion in many cases. Even in semiconductor processes, an adhesion layer of titanium or chromium is commonly used when sputtering gold onto a substrate [38], [39]. The adhesion of the uncapped gold printed onto smooth substrates like polyimide and glass, while resistant to flexing stress, could be easily scratched off. This is unideal for many cases where the gold would be exposed, like sensors or wearables. The plasma jet-printed gold traces did not exhibit good adhesion to relatively smooth substrates like glass, Kapton, and silicon, which could be scratched easily with a probe or gloved hand. Electrodes printed onto paper substrates had much better adhesion, as the surface's roughness increased the surface's coating, as has been previously reported [32].

3.4 Modified gold ink for improved adhesion

A new, modified gold ink (IFL_MJ-Au3) was printed with PJP to test the formulation for increased adhesion. These nanoparticles were modified as described by ref. 37, where much, but not all, of the PVP capping agent is removed by washing. The optimized sheath and precursor flows were determined to be 550 SCCM and 100 SCCM for the new ink, using a 2 mm print height from the substrate. Simple lines for measuring the resistance of the ink were printed with 2 passes at varying plasma voltages from 5.0 to 15kV. Since the ink had trace additives of polymer, ethanol, and Ethylene glycol, a simple pass of plasma over the printed traces was needed to achieve conductivity and remove the polymer and solvent from the deposited film, as has been inferred previously [32]. The capping agent must be removed before the sintering of the nanoparticles occurs. As the particles are exposed to heat and plasma, Oswald ripening will occur when the individual particles form necks and begin to fuse together. This is highlighted in the three SEM images of Fig. 5. Initially at 10kV, there are individual particles that are not very conductive. When the voltage is increased to 15kV, the particles start to fuse together but are in a partial state of sintering. When a 10-pass plasma treatment has been performed, a much more connected network of particles is observed, resulting in a more than 10x drop in resistance. This phenomenon is also observed in the cross-section SEM images as well (Fig. 6a). Low-temperature burn-off polymer and also reducing the amount of polymer in the printed films helps to reduce the sintering temperature required for achieving low-temperature sintering. The lines were treated with 2 passes of only helium plasma with the atomization system turned off. The speed during this treatment step was carried out at 0.1mm/s for best results. To further increase the conductivity of the printed samples, the treatment step was performed at 2-10 passes of the samples printed at 15kV.

IFL_MJ-Au3 was deposited at 0.5 mm/s print speed and at voltages from 5kV to 15kV. These samples were treated with 2 passes of plasma at 0.1 mm/s, without ink atomization, at the

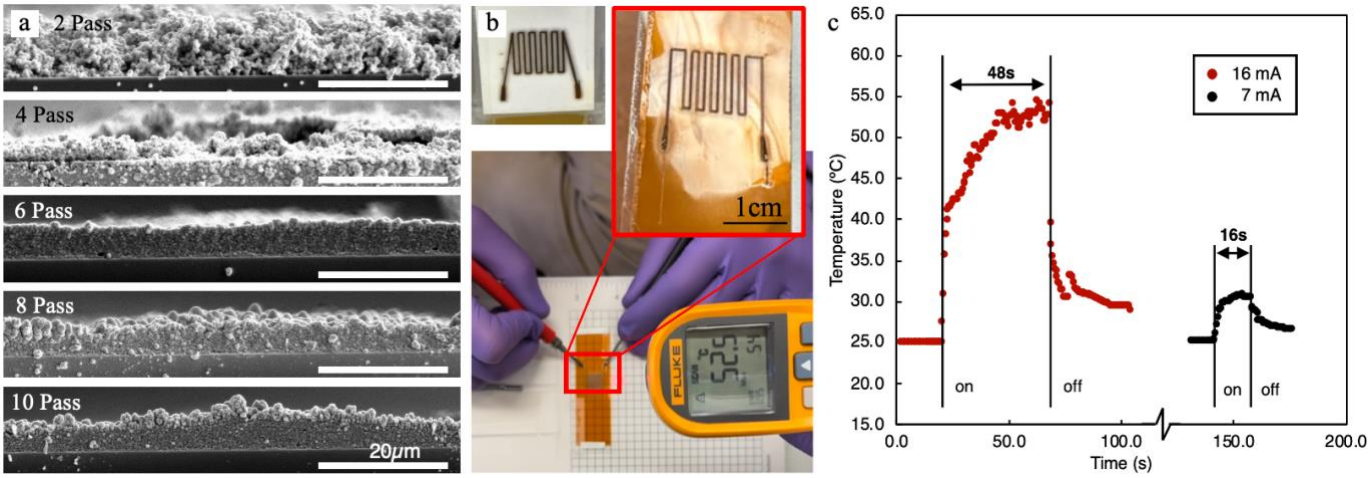

Fig. 6. (a) Cross-sectional SEM of modified gold nanoparticle ink printed at 15kV plasma voltage and treated from 2-10 passes. All scale bars are 20μm. (b) Printed microheater on paper and polyimide. Temperature observed with IR thermometer. (c) Temperature vs time for printed microheater on polyimide with varying current.

same deposition voltage. Electrical resistance measurements were taken of the printed lines, and for the 5kV and 7.5kV depositions, there was no conductivity. From 10kV to 15kV, the resistance of the printed line decreased significantly down to hundreds of ohms. Fig. 5a (left) shows resistance vs. deposition voltage for the capped gold ink. Multiple passes of plasma over the printed gold resulted in a further decrease in the resistance of the printed gold. The average resistance shown in Fig. 5a (right) is for the gold printed at 15kV and treated at 15kV at 0.1mm/s plasma speed. With more plasma treatments, the film's resistance decreases, saturating with more passes up to 10. The error bars represent the standard error of the sample set at each treatment number.

SEM imaging was performed on the samples with each deposition parameter and plasma treatment to understand what was happening to the deposited nanoparticles. Fig. 5b shows SEM images of the deposited gold at 10kV, 15kV, and 15kV with 10 treatment passes. It was observed that at 10kV, again, there is insufficient necking and particle growth for good conductivity. The added polymer must be burned off in order to sinter the nanoparticles through Oswald ripening [13]. When the voltage increased to 15kV then necking and densification between the particles occurs as seen in Fig. 5b. With increased plasma treatment, densification and necking of the nanoparticles further increased. In the SEM images (Fig. 5b), between 2 and 10 plasma passes, significant grain growth is observed so that there are few nanoparticles left, which is consistent of fully sintered nanomaterials [28], [29], [30]. Cross-sectional SEM images were taken of the samples printed at 15kV and treated from 2-10 passes. Significant densification of the gold nanoparticles can be seen as the particles become a more solid film from individual nanoparticles (Fig. 6a). Based on the 0.1 mm/s speed, the printed line sample receives 10 seconds of plasma treatment every millimeter. Since the plasma jet width is less than a millimeter, even at the highest number of plasma treatments, each one-millimeter section receives a maximum of 100 seconds of plasma treatment. This time of just under 2 minutes of constant plasma exposure to the film is significantly improved over the tens of minutes to hours required in previous studies [29], [30], [40].

As multiple passes of plasma treatment are performed, the temperature of the substrate is important to consider. The temperature at the substrate due to atmospheric pressure plasma has been recorded under 60°C when the plasma is used to treat samples in cycles and for several minutes [30], [41]. Particularly when the plasma is cycled on and off or when it is rastered, the local heating on the substrate can stay below 50°C, ensuring the ability to print and sinter on low-temperature substrates. This has been studied for biomedical applications and biofilm treatment, where atmospheric pressure plasma jets are used as they have the benefits of high-temperature plasmas

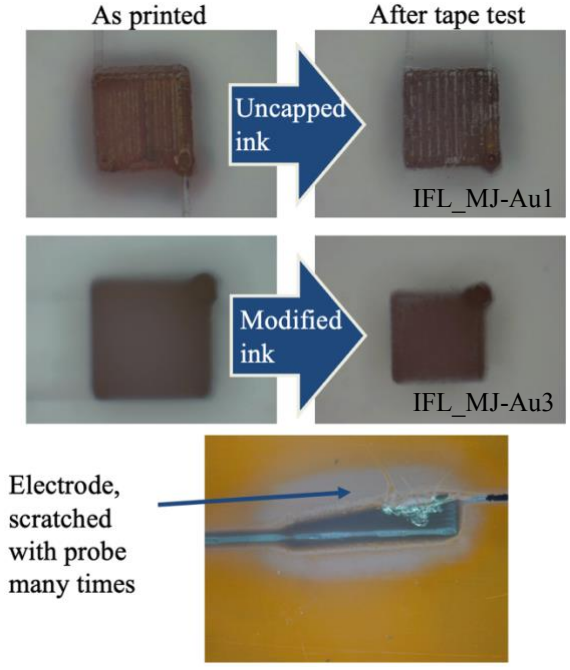

Fig. 7. (Top) IFL_MJ-Au2 and (middle) IFL_MJ-Au3 printed and before and after tape test. (bottom) Electrode end probed many times while remaining well adhered.

but operate at 30-50°C where tissue damage is not an issue [13], [42].

With the modified ink, IFL_MJ-Au3, the adhesion, especially after treatment, was significantly increased. Gold lines and electrodes were not easily scratched off, and the probe could not remove them from the substrate with regular force. When scratched with the probe, the films stayed intact. The surface of the films was roughened as seen in Fig. 7, but the gold was not removed from the substrate. To ensure the NPs were sintered and not removable with solvent, the films were rinsed with DI water isopropyl alcohol, and ethanol from a bottle, which also left the films intact and conductive. Some gold overspray was rinsed off, but the bulk of the film remained unbroken. To test the adhesion to tape force, gold pads were also printed with both inks, and a fresh piece of 3M Scotch tape was applied by hand. A basic tape test with 90º pull-off was performed by gripping the one end of the tape and pulling slowly and a perpendicular direction to the substrate. The adhesion test was quantified by observing the prints optically before and after the scotch tape test to see how much of the film was removed. This can be seen in Fig. 7. Visible gold removal is seen in the uncapped ink pad. With the modified ink, IFL_MJ-Au3, there was some gold removed, but the underlying print maintained its conductivity while the uncapped ink did not retain conductivity (Fig. 7). The film, as seen in the image after tape tests, remains attached to the glass substrate. The lines printed and post-plasma treated did not reveal any reduction in flexibility, as LED electrodes printed with both setups could be flexed without loss of brightness of the LED.

3.5 Printed heater

To demonstrate the performance of gold deposited using plasma jet printing in this method, a printed microheater was fabricated with the modified gold ink. Microheaters have been fabricated using traditional and additive manufacturing techniques, with some complicated fabrication techniques, but have not been demonstrated using plasma-jet printing technology [43], [44], [45], [46], [47]. Gold microheaters are crucial in biomedical applications, point-of-care diagnostics, and in flexible, wearable technologies [44], [45], [46]. The plasma jet-printed film exhibited superior adhesion to the substrate, and flexibility and was fabricated using the single tool, single-step PJP process. The gold ink IFL_MJ-Au3 was deposited and treated with the plasma post-deposition to sinter the nanoparticles and remove the slight amount of remaining polymer. Fig. 6b shows one printed microheater onto paper and polyimide. Its temperature response, measured by an IR thermometer with two driven currents applied, is shown in Fig. 6c. The temperature increases quickly when the current is applied and corresponds to the amplitude of the current.

IV. Conclusions

We report the first demonstration of self-sintered and enhanced adhesion with plasma jet-printed gold nanoparticle ink for flexible hybrid electronic applications. Compared to other low-temperature sintering techniques, plasma-jet printing has the major advantage of being a single deposition and sintering tool with no need to move the substrate between a printing and sintering tool, reducing the footprint of end-to-end manufacturing. This is especially crucial for in-space manufacturing and instances where a cleanroom or inert environment may be required. PJP also is rapid and scalable, where larger or multiple plasma sources can further increase sintering speed. While silver nanoparticles can sinter at lower temperatures and have seen better results in terms of conductivity from PJP, gold is required for applications where stability from oxidation and biocompatibility are crucial. While the presented work shows results not achieved previously, further improvements in the conductivity of the gold can open up this method to a wider range of electronic applications. Further study on adhesion and improvements to the resolution of the plasma printhead by using smaller nozzles, could also open the applicability of PJP for flexible hybrid electronics. In this work, gold nanoparticles were deposited onto glass, polyimide, and paper substrates, and the films were self-sintered as they printed. The plasma voltage was varied, and the conductivity and porosity of the printed films were measured. The porosity increased as plasma power increased, and the conductivity peaked at 6.2 $x10^5$ S/m where porosity was minimal and cross-sectional area plots intersect. For increased adhesion, a modified ink was created optimized for the plasma jet. As further plasma passes were performed on the modified ink, the densification and sintering were increased as confirmed by SEM. The resistance of the as-printed lines was also reduced from 190Ω to 15Ω with increased plasma treatment at 15kV plasma voltage. After deposition and a plasma treatment step, conductive films with high adhesion and resistance to scratching were produced from PJP compatible with low-temperature substrates.

References

[1] K. Chang, Y. H. Kim, Y. J. Kim, and Y. J. Yoon, "Functional antenna integrated with relative humidity sensor using synthesised polyimide for passive RFID sensing," *Electron Lett*, vol. 43, no. 5, p. 259, 2007, doi: 10.1049/el:20073739.

[2] V. R. Marinov *et al.*, "Direct-Write Vapor Sensors on FR4 Plastic Substrates," *Ieee Sens J*, vol. 7, no. 6, pp. 937–944, 2007, doi: 10.1109/jsen.2007.895964.

[3] F. Loffredo, G. Burrasca, L. Quercia, and D. D. Sala, "Gas Sensor Devices Obtained by Ink-jet Printing of Polyaniline Suspensions," *Macromol Symp*, vol. 247, no. 1, pp. 357–363, 2007, doi: 10.1002/masy.200750141.

[4] H. Subbaraman *et al.*, "Inkjet-Printed Two-Dimensional Phased-Array Antenna on a Flexible Substrate," *Ieee Antenn Wirel Pr*, vol. 12, pp. 170–173, 2013, doi: 10.1109/lawp.2013.2245292.

[5] D. Huang, F. Liao, S. Molesa, D. Redinger, and V. Subramanian, "Plastic-Compatible Low Resistance Printable Gold Nanoparticle Conductors for Flexible Electronics," *J Electrochem Soc*, vol. 150, no. 7, p. G412, 2003, doi: 10.1149/1.1582466.

[6] S. B. Fuller, E. J. Wilhelm, and J. M. Jacobson, "Ink-Jet Printed Nanoparticle Microelectromechanical Systems," *J Microelectromech S*, vol. 11, no. 1, p. 54, 2002, doi: 10.1109/84.982863.

[7] S. Gamerith, A. Klug, H. Scheiber, U. Scherf, E. Moderegger, and E. J. W. List, "Direct Ink-Jet Printing of Ag–Cu Nanoparticle and Ag-Precursor Based Electrodes for OFET Applications," *Adv Funct Mater*, vol. 17, no. 16, pp. 3111–3118, 2007, doi: 10.1002/adfm.200600762.

[8] D. Kim, S. Jeong, S. Lee, B. K. Park, and J. Moon, "Organic thin film transistor using silver electrodes by the ink-jet printing technology," *Thin Solid Films*, vol. 515, no. 19, pp. 7692–7696, 2007, doi: 10.1016/j.tsf.2006.11.141.

[9] S. H. Ko, J. Chung, H. Pan, C. P. Grigoropoulos, and D. Poulikakos, "Fabrication of multilayer passive and active electric components on polymer using inkjet printing and low temperature laser processing," *Sensors Actuators Phys*, vol. 134, no. 1, pp. 161–168, 2007, doi: 10.1016/j.sna.2006.04.036.

[10] J. Manzi *et al.*, "Plasma-jet printing of colloidal thermoelectric Bi 2 Te 3 nanoflakes for flexible energy harvesting," *Nanoscale*, vol. 15, no. 14, pp. 6596–6606, 2023, doi: 10.1039/d2nr06454e.

[11] N. McKibben *et al.*, "Aerosol jet printing of piezoelectric surface acoustic wave thermometer," *Microsystems Nanoeng*, vol. 9, no. 1, p. 51, 2023, doi: 10.1038/s41378-023-00492-5.

[12] T. Pandhi *et al.*, "Fully inkjet-printed multilayered graphene-based flexible electrodes for repeatable electrochemical response," *Rsc Adv*, vol. 10, no. 63, pp. 38205–38219, 2020, doi: 10.1039/d0ra04786d.

[13] U. Caglar, K. Kaija, and P. Mansikkamaki, "Analysis of mechanical performance of silver inkjet-printed structures," presented at the 2008 2nd IEEE International Nanoelectronics Conference, in Nanomaterials, vol. 10. 2008, pp. 851–856. doi: 10.1109/inec.2008.4585617.

[14] X. Lin, T. Ling, H. Subbaraman, L. J. Guo, and R. T. Chen, "Printable thermo-optic polymer switches utilizing imprinting and ink-jet printing," *Opt. Express*, vol. 21, no. 2, p. 2110, 2013, doi: 10.1364/oe.21.002110.

[15] A. Kamyshny and S. Magdassi, "Conductive nanomaterials for 2D and 3D printed flexible electronics," *Chem. Soc. Rev.*, vol. 48, no. 6, pp. 1712–1740, 2018, doi: 10.1039/c8cs00738a.

[16] Q. Huang and Y. Zhu, "Printing Conductive Nanomaterials for Flexible and Stretchable Electronics: A Review of Materials, Processes, and Applications," *Advanced Materials Technologies*, vol. 4, no. 5, p. 1800546, 2019, doi: 10.1002/admt.201800546.

[17] A. Kamyshny and S. Magdassi, "Conductive Nanomaterials for Printed Electronics," *Small*, vol. 10, no. 17, pp. 3515–3535, 2014, doi: 10.1002/smll.201303000.

[18] "Precedence Research , 'Printed electronics market - global industry analysis, size, share, growth, trends, regional outlook, and forecast 2021 - 2030,' Globe NewsWire, 18-Nov-2021. [Online]. Available: https://www.precedenceresearch.com/printed-electronics-market. [Accessed: 18-Apr-2022].".

[19] K. Rajan, I. Roppolo, A. Chiappone, S. Bocchini, D. Perrone, and A. Chiolerio, "Silver nanoparticle ink technology: state of the art," *Nanotechnology, Science and Applications*, vol. 9, pp. 1–13, Dec. 2016, doi: 10.2147/nsa.s68080.

[20] N. Turan, P. M. Barboun, P. K. Nayak, J. C. Hicks, and D. B. Go, "Development of a small-scale helical surface dielectric barrier discharge for characterizing plasmasurface interfaces," *J. Phys. D: Appl. Phys.*, vol. 53, no. 27, p. 275201, 2020, doi: 10.1088/1361-6463/ab8320.

[21] M. Zenou and L. Grainger, "3 - Additive manufacturing of metallic materials," ["Jing Zhang" and "Yeon-Gil Jung"], Eds., Butterworth-Heinemann, 2018, pp. 53–103. doi: 10.1016/b978-0-12-812155-9.00003-7.

[22] W. Cui, W. Lu, Y. Zhang, G. Lin, T. Wei, and L. Jiang, "Gold nanoparticle ink suitable for electric-conductive pattern fabrication using in ink-jet printing technology," vol. 358, no. 1, pp. 35–41, Apr. 2010, doi: 10.1016/j.colsurfa.2010.01.023.

[23] S. Mekhmouken *et al.*, "Gold nanoparticle-based eco-friendly ink for electrode patterning on flexible substrates," *Electrochem. Commun.*, vol. 123, p. 106918, 2021, doi: 10.1016/j.elecom.2021.106918.

[24] Y. Wu, Y. Li, B. S. Ong, P. Liu, S. Gardner, and B. Chiang, "High-Performance Organic Thin-Film Transistors with Solution-Printed Gold Contacts," *Adv. Mater.*, vol. 17, no. 2, pp. 184–187, 2005, doi: 10.1002/adma.200400690.

[25] N. P. Bacalzo, L. P. Go, C. J. Querebillo, P. Hildebrandt, F. T. Limpoco, and E. P. Enriquez, "Controlled Microwave-Hydrolyzed Starch as a Stabilizer for Green Formulation of Aqueous Gold Nanoparticle Ink for Flexible Printed Electronics," *ACS Appl. Nano Mater.*, vol. 1, no. 3, pp. 1247–1256, 2018, doi: 10.1021/acsanm.7b00379.

[26] S. H. Ko, H. Pan, C. P. Grigoropoulos, C. K. Luscombe, J. M. J. Fréchet, and D. Poulikakos, "All-inkjet-printed flexible electronics fabrication on a polymer substrate by low-temperature high-resolution selective laser sintering of metal nanoparticles," *Nanotechnology*, vol. 18, no. 34, p. 345202, 2007, doi: 10.1088/0957-4484/18/34/345202.

[27] A. Albrecht, A. Rivadeneyra, A. Abdellah, P. Lugli, and J. F. Salmerón, "Inkjet printing and photonic sintering of silver and copper oxide nanoparticles for ultra-low-cost conductive patterns," *J. Mater. Chem. C*, vol. 4, no. 16, pp. 3546–3554, 2016, doi: 10.1039/c6tc00628k.

[28] J. Niittynen, R. Abbel, M. Mäntysalo, J. Perelaer, U. S. Schubert, and D. Lupo, "Alternative sintering methods compared to conventional thermal sintering for inkjet printed silver nanoparticle ink," vol. 556, pp. 452–459, Apr. 2014, doi: 10.1016/j.tsf.2014.02.001.

[29] I. Reinhold *et al.*, "Argon plasma sintering of inkjet printed silver tracks on polymer substrates," *J Mater Chem*, vol. 19, no. 21, pp. 3384–3388, 2009, doi: 10.1039/b823329b.

[30] N. Turan, M. Saeidi-Javash, J. Chen, M. Zeng, Y. Zhang, and D. B. Go, "Atmospheric Pressure and Ambient Temperature Plasma Jet Sintering of Aerosol Jet Printed Silver Nanoparticles," *Acs Appl Mater Inter*, vol. 13, no. 39, pp. 47244–47251, 2021, doi: 10.1021/acsami.1c14049.

[31] R. Ramamurti *et al.*, "Atmospheric Pressure Plasma Printing of Nanomaterials for <italic>IoT</italic> Applications," *Ieee Open J Nanotechnol*, vol. 1, no. 99, pp. 47–56, 2020, doi: 10.1109/ojnano.2020.3009882.

[32] J. Manzi, N. Kandadai, R. P. Gandhiraman, and H. Subbaraman, "Plasma Jet Printing: An Introduction," *Ieee T Electron Dev*, pp. 1–6, 2023, doi: 10.1109/ted.2023.3248526.

[33] D. H. Gutierrez, P. Doshi, D. Nordlund, and R. P. Gandhiraman, "Plasma jet printing of metallic patterns in zero gravity," *Flexible Print Electron*, vol. 7, no. 2, p. 25016, 2022, doi: 10.1088/2058-8585/ac73cb.

[34] S. Khan, T. P. Nguyen, L. Thiery, P. Vairac, and D. Briand, "Aerosol Jet Printing of Miniaturized, Low Power Flexible Micro-Hotplates," *Proceedings*, vol. 1, no. 4, p. 316, 2017, doi: 10.3390/proceedings1040316.

[35] Ph. Buffat and J.-P. Borel, "Size effect on the melting temperature of gold particles," *Phys. Rev. A*, vol. 13, pp. 2287–2298, 1976, doi: 10.1103/physreva.13.2287.

[36] R. P. Gandhiraman, E. Singh, D. C. Diaz-Cartagena, D. Nordlund, J. Koehne, and M. Meyyappan, "Plasma jet printing for flexible substrates," *Appl Phys Lett*, vol. 108, no. 12, p. 123103, 2016, doi: 10.1063/1.4943792.

[37] T. V. Varghese *et al.*, "Multijet Gold Nanoparticle Inks for Additive Manufacturing of Printed and Wearable Electronics," *ACS Mater. Au*, 2023, doi: 10.1021/acsmaterialsau.3c00058.

[38] J. C. Hoogvliet and W. P. van Bennekom, "Gold thin-film electrodes: an EQCM study of the influence of chromium and titanium adhesion layers on the response," *Electrochim Acta*, vol. 47, no. 4, pp. 599–611, 2001, doi: 10.1016/s0013-4686(01)00793-9.

[39] H. Savaloni, A. Taherizadeh, and A. Zendehnam, "Residual stress and structural characteristics in Ti and Cu sputtered films on glass substrates at different substrate temperatures and film thickness," *Phys B Condens Matter*, vol. 349, no. 1–4, pp. 44–55, 2004, doi: 10.1016/j.physb.2004.01.158.

[40] N. Turan, M. Saeidi-Javash, Y. Zhang, and D. B. Go, "Does plasma jet sintering follow an Arrhenius-type expression?," *Plasma Process Polym*, vol. 19, no. 8, p. 2200011, 2022, doi: 10.1002/ppap.202200011.

[41] S. Wünscher *et al.*, "Localized atmospheric plasma sintering of inkjet printed silver nanoparticles," *J. Mater. Chem.*, vol. 22, no. 47, pp. 24569–24576, 2012, doi: 10.1039/c2jm35586h.

[42] O. V. Penkov, M. Khadem, W.-S. Lim, and D.-E. Kim, "A review of recent applications of atmospheric pressure plasma jets for materials processing," *J. Coat. Technol. Res.*, vol. 12, no. 2, pp. 225–235, 2015, doi: 10.1007/s11998-014-9638-z.

[43] H. Al-Mohsin, S. Ali, and A. Bermak, "Design and Fabrication Process Optimization of Silver-Based Inkjet-Printed Microheater," *Processes*, vol. 10, no. 9, p. 1677, 2022, doi: 10.3390/pr10091677.

[44] Z. E. Jeroish, K. S. Bhuvaneshwari, F. Samsuri, and V. Narayanamurthy, "Microheater: material, design, fabrication, temperature control, and applications—a role in COVID-19," *Biomed. Microdevices*, vol. 24, no. 1, p. 3, 2022, doi: 10.1007/s10544-021-00595-8.

[45] K. M. Byers, L.-K. Lin, T. J. Moehling, L. Stanciu, and J. C. Linnes, "Versatile printed microheaters to enable low-power thermal control in paper diagnostics," *Analyst*, vol. 145, no. 1, pp. 184–196, 2019, doi: 10.1039/c9an01546a.

[46] A. VanHorn and W. Zhou, "Design and optimization of a high temperature microheater for inkjet deposition," *Int. J. Adv. Manuf. Technol.*, vol. 86, no. 9–12, pp. 3101–3111, 2016, doi: 10.1007/s00170-016-8440-8.

[47] M. Gregorini, R. N. Grass, and W. J. Stark, "One-Step Photolithographic Surface Patterning of Nanometer-Thick Gold Surfaces by Using a Commercial DLP Projector and the Fabrication of a Microheater," *Ind. Eng. Chem. Res.*, vol. 59, no. 26, pp. 12048–12055, 2020, doi: 10.1021/acs.iecr.9b05837.